Polymer Vol. 39 No. 22, pp. 5283–5291, 1998

0032-3861/98/$ - see front matter

PII: S0032-3861(97)10295-6

polymer papers

Polyethylene (PEHD)/polypropylene (iPP) blends: mechanical properties, structure and morphology

B. L. Schürmann[a,*], U. Niebergall[a], N. Severin[a], Ch. Burger[b], W. Stocker[c] and J. P. Rabe[c]

[a]*Bundesanstalt für Materialforschung und -prüfung, Unter den Eichen 87, 12205 Berlin, Germany*
[b]*Max-Planck-Institut für Kolloid- und Grenzflächenforschung, Kantstr. 55, 14153 Teltow, Germany*
[c]*Humboldt-Universität zu Berlin, Institut für Physik, Invalidenstr. 110, 10115 Berlin, Germany*
(Received 24 July 1997; accepted 5 November 1997)

High density polyethylene (PEHD) and isotactic polypropylene (iPP) blends exhibit a maximum in impact strength at a specific mixing ratio. This effect is even more pronounced if a compatibilizer is added. An explanation was found by analyzing the morphology. From scanning force microscopy results on samples crystallized from the melt it can be concluded that mixing of iPP with PEHD causes a decrease of iPP spherulite size as compared to pure iPP. After processing such an extrusion and quenching no spherulites but an excellent distribution of nucleation centres was found by transmission electron microscopy, indicating an increase of the total interphasial volume within the blend material, which in turn improves the impact strength. On the microscopic level the energetically most favourable interphasial molecular arrangements are obtained by molecular dynamics calculations.

(Keywords: PEHD/iPP blends; mechanical properties; structure and morphology)

INTRODUCTION

Polyethylene and polypropylene are of considerable industrial relevance, especially in the form of a blend. Mechanical properties such as impact strength, tensile strength, Young's modulus, strength and elongation at the stretching limit as well as processing properties need to be optimized. In general, in systems of two polymers the tensile strength can depend linearly on the concentration of one component, but antagonistic and synergistic effects have also been reported[1]. Incompatible and immiscible polymers may exhibit a broad minimum in tensile strength over the composition[2]. The term 'immiscible' means that the Gibbs free energy of mixing ΔG_m is positive, whereas 'incompatible' is defined with respect to properties and means that the properties of the blend are inferior to those of the pure polymers. Since polyethylene and polypropylene are generally immiscible and incompatible[3,4], their mixtures are expected to be poor in mechanical properties. However, the high density polyethylene (PEHD)/isotactic polypropylene (iPP) blend is one of the few immiscible systems which has a maximum in tensile strength for a certain composition[5], i.e. it is not incompatible. Moreover, addition of a small amount of PEHD into iPP improves the impact strength of iPP[6], and addition of a small amount of iPP into PEHD enhances transparency of solid PE[7] (at the expense of environmental stress cracking resistance). These effects depend on the blend preparation conditions. In order to put the blends into effective and efficient use, a study is needed to understand their structure, properties, and processing behaviour.

In our PEHD/iPP blend samples a surprisingly high impact strength compared to the single components is observed at a specific range of PEHD content. This phenomenon raises questions as to the structure, morphology and the interphases between the components and their possible correlation with the impact strength. To study this, several methods such as scanning force microscopy (SFM), transmission force microscopy (TEM), wide-angle X-ray scattering (WAXS), small-angle X-ray scattering (SAXS) and molecular dynamics (MD) calculations were applied.

EXPERIMENTAL

iPP and PEHD were obtained from Hoechst AG. They were characterized as follows. iPP: melting point 165°C, number average molecular weight M_n = 480 000 g/mol, density 0.902 g/cm^3, melting flow index 0.6 g/10 min; PEHD: melting point 128°C, number average molecular weight M_n = 215 000 g/mol, density 0.943 g/cm^3, melting flow index 0.4 g/10 min. The blend samples were prepared by a single screw extruder from the melt; the PEHD content varied from 5 to 95 wt% in steps of 5 wt%. The melt was pressed into injection moulded test pieces and then rapidly cooled in a water bath. It is worth mentioning that the injection moulded samples of the pure PEHD and iPP were not treated by extrusion before moulding.

* To whom correspondence should be addressed: c/o Prof. J. P. Rabe, Humboldt-Universität zu Berlin, Institut für Physik, Invalidenstr. 110, 10115 Berlin, Germany

Injection moulding of test pieces was performed according to ISO/DIS 3167 Type A. The notched impact test was carried out according to ISO 179, the tensile test according to DIN 54455.

For SFM, thin films of iPP, PEHD and iPP/PEHD blends were solution cast onto glass cover slides by evaporation of the solvent of a dilute solution (0.1% w/v) of the polymer at 150°C in xylene. After evaporation of the solvent the molten thin film was recrystallized by cooling at a controlled rate (−20°C/min). Etching of the injection moulded sample was performed in a mixture of 1.3 wt% $KMnO_4$/32.9 wt% H_3PO_4/65.8 wt% H_2SO_4 for 18 h.

SFM experiments were carried out with a Nanoscope III microscope (Digital Instruments Inc., Santa Barbara, CA) in the tapping mode, where the change of the tip oscillation amplitude is detected, which is introduced by touching the sample surface periodically. Si cantilevers (length = 125 μm, width = 30 μm, thickness = 3–5 μm) with a spring constant in the range 17–64 N/m and a resonance frequency in the range of 240–400 kHz were used. In tapping mode operation, lateral shear forces are minimized when the cantilever is oscillating close to the resonance frequency. Resonance peaks in the frequency response of the cantilever, typically in the range 280–320 kHz, were chosen for the tapping mode oscillation. Vibration amplitudes usually in the range 20–30 nm were applied. The SFM images were obtained with a J-type scan head (maximum scan range 150 μm × 150 μm). The amplitude of the oscillation was calibrated with respect to the vertical position of the piezoelectric scanner. Imaging was performed displaying the amplitude signal (incoming signal for the feedback system) and the height signal (output of the feedback system). Feedback parameters were optimized by minimizing changes in the amplitude signal. All images presented are height images. Scanning line frequencies were usually between 0.5 and 2 Hz. The measurements were carried out in air under normal conditions.

Two-dimensional WAXS patterns have been recorded using a Paar PHK pinhole camera with imaging plates and a DIP3000 imaging plate scanner (direction of injection is vertical, sample–director distance 60 mm, 0.4 mm pinholes, in vacuum, IP pixelsize 100 μm, Cu K_α radiation at 30 kV and 40 mA, Ni filter, exposure 30 min). SAXS curves are taken with a Paar Kratky compact camera and a Braun linear position-sensitive detector only.

MOLECULAR MODELLING

Amorphous cells were constructed from 18 molecules containing 40 residues of PEHD and 16 molecules consisting of 30 residues of iPP. Each of the molecular chains was energy minimized by the molecular mechanics and molecular dynamics method[8]. Inter- and intramolecular interactions are described by the potential given in the following:

$$
\begin{aligned}
E_{\text{pot}} = & \sum_b \left[K(b-b_0)^2\right] + \sum_\theta (\theta-\theta_0)^2 \\
& + \sum_\varphi V\left[1+\cos(\varphi-\varphi_1^0)\right] + \sum_\chi K_\chi \chi^2 \\
& + \sum_b \sum_{b'} F_{bb'}(b-b_0)(b'-b_0{}') \\
& + \sum_\theta \sum_{\theta'} F_{\theta\theta'}(\theta-\theta_0)(\theta'-\theta_0{}') \\
& + \sum_b \sum_\theta F_{b\theta}(b-b_0)(\theta-\theta_0) \\
& + \sum_b \sum_\varphi (b-b_0)\left[V_1\cos\varphi + V_2\cos 2\varphi + V_3\cos 3\varphi\right] \\
& + \sum_{b'} \sum_\varphi (b'-b'_0)\left[V_1\cos\varphi + V_2\cos 2\varphi + V_3\ \cos 3\varphi\right] \\
& + \sum_\theta \sum_\varphi (\theta-\theta_0)\left[V_1\cos\varphi + V_2\cos 2\varphi + V_3\cos 3\varphi\right] \\
& + \sum_\varphi \sum_\theta \sum_\theta K_{\varphi\theta\theta'}\cos\varphi(\theta-\theta_0)(\theta'-\theta_0') \\
& + \sum_{i>j} \frac{q_i q_j}{\epsilon r_{oj}} + \sum_{i>j}\left[\frac{A_{ij}}{r_{ij}^9} - \frac{B_{ij}}{r_{ij}^6}\right] \qquad (1)
\end{aligned}
$$

The force field parameters are taken from the pcff force field of the Biosym polymer package[8]. Creation of the amorphous bulk state requires the single chains packed into a unit cell, which is infinitely repeated by periodic boundary conditions with an experimentally given density of 0.85 g/cm^3 for iPP and also PEHD. In order to obtain reasonable statistics, 18 molecules in the case of PEHD and 16 molecules in the case of iPP were packed into the periodic boundary conditions (p.b.c.) box; during the packing procedure the neighbourhood of each atom is checked by distance criteria: the sum of the van der Waals radii must be the minimum distance between two nonbonded atoms. The size of the boxes were chosen to be more than 1.9 nm to allow a cut off distance of 0.95 nm. This structure is then prerelaxed by 1000 steps of conjugated gradient energy minimization using the full potential given in equation (1) to remove bad contacts. In order to optimize the sample further the system was subjected to annealing cycles of 20 ps duration where the temperature is decreased linearly from 800 to 300 K. After 3 cycles there was no further decrease of the potential energy. The MD simulations for the NVT ensemble were performed using the leap-frog algorithm with a time step of 1 fs. The temperature T is kept constant at 300 K according to the loose coupling algorithm of Berendsen *et al.*[9]. The MD runs were performed over 200 ps and frames of the trajectory were stored every 1 ps.

The crystalline cells were constructed by adopting the orthorhombic unit cell of PE and the α-form unit cell of iPP[10]. The smallest dimension of the final cell was greater than 1.9 nm. After energy minimization the crystalline samples were annealed for 20 ps at temperatures decreasing from 500 to 300 K in steps 50 K. Heating to over 500 K caused gauche defects in PE and a higher potential energy.

Amorphous/amorphous and crystalline/amorphous interfaces were constructed by layering of the PEHD and iPP ensembles. For the crystalline/crystalline interface four different models were created, depending on the angle between the molecular iPP and PEHD chain axes: 0°, 90°, 46.8° and −46.8°. To obtain the thickness of the interphases the ensembles described above were augmented by a slice of benzene molecules (20 nm thick). This additional layer screens the effect caused by the periodic boundary conditions. Each of the combined systems were subjected to MD simulations for the NPT ensemble using the leap-frog algorithm with a time step of 1 fs. The temperature T was kept constant at 300 K by the loose coupling algorithm of Berendsen *et al.*[9]. The pressure (P = 1 bar) was controlled by the Parrinello–Rahman method[11]. The total simulation

time after relaxation was 500 ps for each crystalline/crystalline ensemble.

Adhesion energies of the PEHD/iPP interfaces were calculated according to:

$$E_{adh} = \frac{E_1 + E_2 - E_c - E_{1surf} - E_{2surf}}{S}$$

where E_{adh} is adhesion energy, E_1 and E_2 are the energies of each component building the system, E_c is the energy of the combined system, E_{1surf} and E_{2surf} are the surface energies of the first and second component and S is the area of the interface.

RESULTS AND DISCUSSION

Mechanical properties

Young's moduli were measured for blends with a wide range of compositions. Evidently their values follow the mixing rule over the whole range (*Figure 1*) and the compatibilizer has almost no effect.

The impact strength, however, exhibits a very pronounced deviation from a simple linear dependence (*Figure 2*). For a mixing ratio of 60% PEHD/40% iPP the impact strength is twice as high as for the single component iPP. For the blends containing a compatibilizer (ethylene–propylene copolymer) the impact strength becomes five times higher than that of iPP and ten times higher than that of PEHD. This phenomenon must be due to an improved energy dissipation, which is correlated to the structure, morphology and interphases within the material. Because the material containing the compatibilizer is more difficult to investigate, we concentrated on the two-component blend.

Scanning force microscopy

Analysis of the obtained SFM images shows different iPP spherulite sizes depending on the crystallization conditions: for the pure iPP film one obtains a spherulite size with a diameter of about 70–150 μm (*Figure 3*). The film prepared from the 50/50 iPP/PEHD blend (*Figure 4*) still shows the typical spherulite form of iPP, but the diameter of the spherulites is decreased (about 30 μm). PEHD nanocrystallites are found on top and inside the iPP spherulites. This interpretation is based on the comparison of the SFM images of the pure iPP film and the pure PEHD film. The SFM image of the compression moulded iPP sample after etching treatment shows a spherulite size of about 15 μm (*Figure 5*). This decrease of spherulite size is attributed to the quenching process performed on the test pieces. In the compression moulded sample of the 50/50 iPP/PEHD blend after etching we cannot recognize any iPP spherulites.

Transmission electron microscopy

Microtome sectioned injection moulded test pieces of the pure materials as well as of the blends were stained by RuO_4 and imaged by TEM. The pure iPP sample shows clearly the typical spherulites as recognized by SFM. Their diameter is approximately 15 μm. In the PEHD sample on the same scale pronounced spherulites are hardly detectable; instead, one finds domains without inner structure.

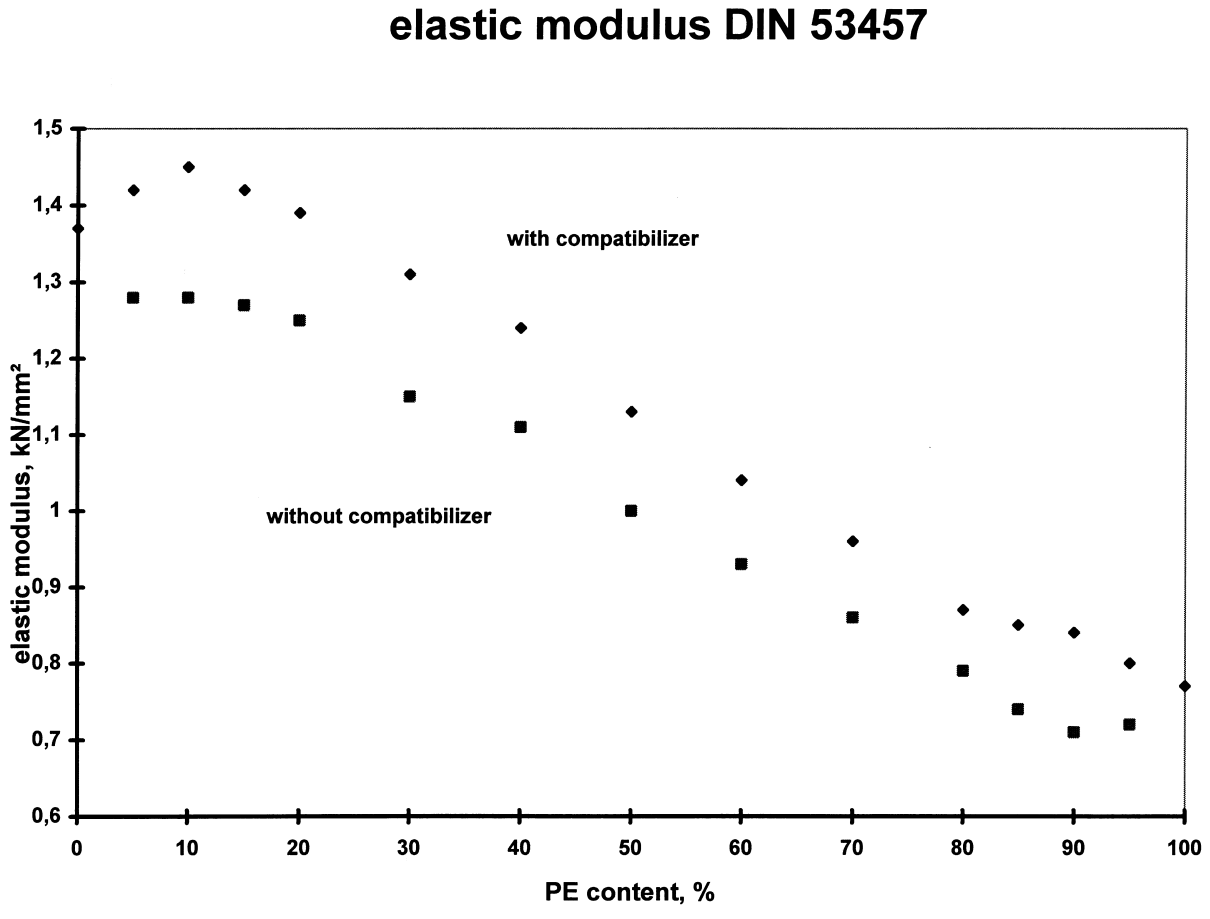

Figure 1 Young's modulus of different blend samples dependent on the PE content without compatibilizer (■) and with compatibilizer (♦). The measurement was carried out according to DIN 53452

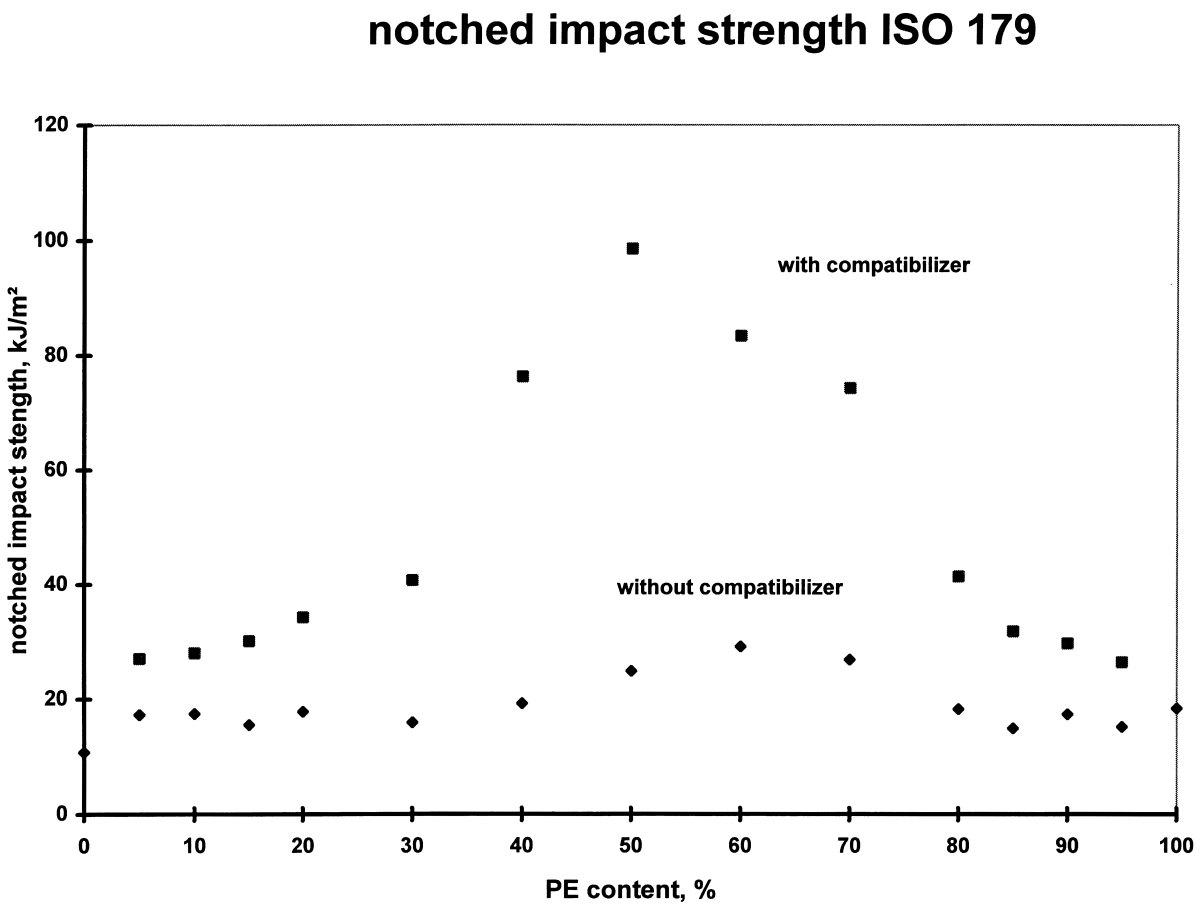

Figure 2 Impact strength as a function of PEHD content without (♦) and with (■) compatibilizer measured according to ISO 179. For a mixing ratio of 60% PEHD/40% iPP the impact strength is twice as high as for the pure iPP. For the blends containing the compatibilizer the a_k value becomes five times higher than the one of pure PEHD and ten times higher than the one of pure iPP

Upon analysing the TEM micrograph of the blend sample (*Figure 6a*) one finds PEHD domains (darker contrast) of about 400–800 nm included in an iPP network (brighter contrast).

The iPP network is still built up by the well known crosshatched structure. In comparison the PEHD lamellae seem to be more disordered and show a more pronounced curvature. The images on the 1 μm scale appear as a continuous network of iPP surrounding domains of PEHD. The PEHD lamellae thickness is estimated to about 8 nm. This dimension is found both in the blend sample as well as in the pure material (*Figure 6b*). The micrograph with the

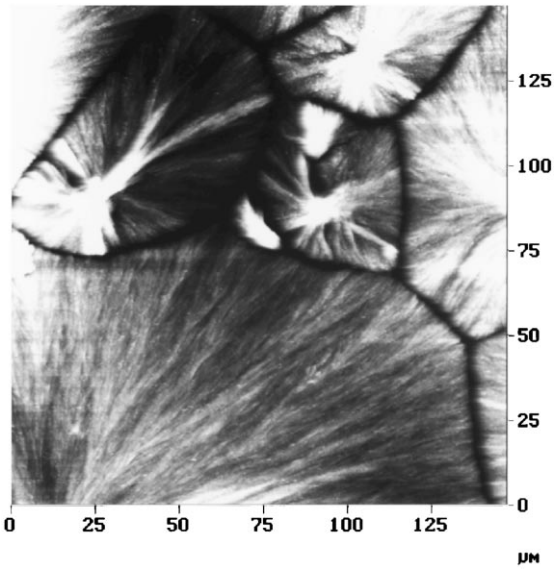

Figure 3 SFM image of pure iPP spherulites within a thin film prepared by solution casting on glass cover slides (z-scale 400 nm)

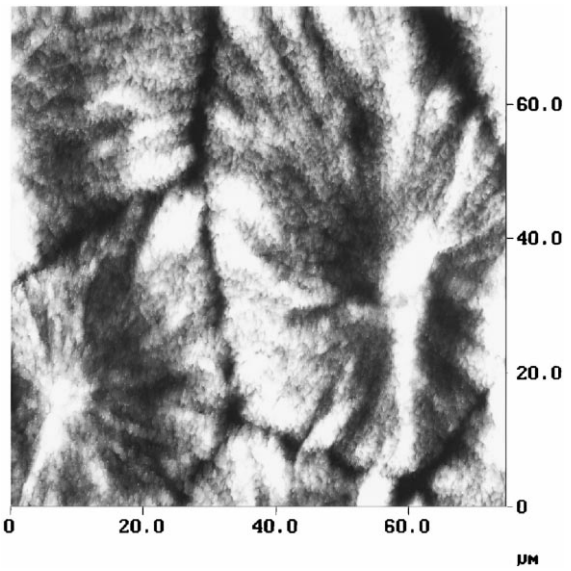

Figure 4 SFM image of a thin film prepared from a 50/50 iPP/PEHD blend (z-scale 250 nm). The typical spherulitic form of iPP is still present, but the diameter has decreased

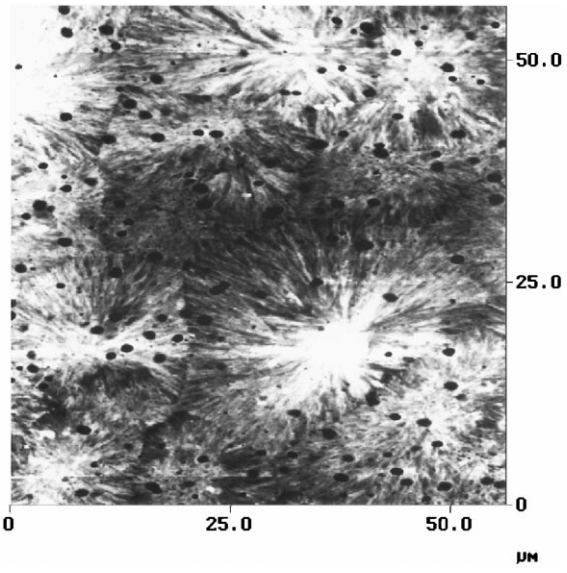

Figure 5 SFM image of the compression moulded iPP sample after etching treatment (*z*-scale 400 nm): compared to the iPP spherulites within the thin film the spherulite size is significantly smaller

smallest magnification displays a very fine dispersion of both components. The typical perfectly grown iPP spherulites do not exist, contrary to the pure iPP sample. At this point we conclude separation between PEHD and iPP takes place at the micrometer scale.

From SFM and TEM results it can be concluded that the pure interaction of iPP with PEHD causes a decrease of spherulite size in iPP. Technical treatment such as extrusion supports an excellent distribution of the nucleation centers. Finally the total interphasial volume within the blend material is increased significantly, leading to an improved impact strength.

X-ray scattering

The two pure samples as well as the 50/50 blend show the typical scattering of a semi-crystalline polymer consisting of sharp crystalline reflections and an amorphous halo. As can be clearly observed in the scattering diagrams, the injection molding process induced a considerable amount of preferred orientation in the samples.

The PEHD shows a typical scattering pattern (*Figure 7a*) indicating the presence of a preferred *b*-axis orientation, i.e. the crystallographic *b*-axis of the PEHD unit call is preferably oriented in the plane normal to the injection direction, and the *a*- and *c*-axes are uniformlly distributed about it. This kind of orientation is typical for polyethylene crystallizing from a melt under not too strong a stretching. The iPP sample (*Figure 7b*) shows a common *c*-axis orientation with the crystallographic *c*-axis, i.e. the direction of the polymer chains preferably oriented in the injection direction. The scattering diagram (*Figure 7c*) of the PEHD/iPP blend sample shows a more or less unperturbed superposition of the scattering patterns of the pure samples. All the crystalline reflections but no additional reflections are found.

It has been verified for an equatorial section of the reciprocal space using a diffractometer with a PDS120 curved position sensitive detector that there is no significant difference in the peak width between the pure samples and the blends. Thus, it can be concluded that at least the crystalline regions of the blend consist of either pure PEHD or pure iPP and have a size comparable to the size in the pure compounds.

Interestingly enough, the unperturbed superposition of features in the scattering diagram of the blend also holds for the different types of orientation observed in the PEHD and iPP domains, preferred *b*-axis and *c*-axis orientation, respectively.

It is concluded that the separation between PEHD and iPP takes place on a fairly large scale since otherwise it is difficult to see how the different domains could retain their respective orientations or how the row nucleation process to which the *b*-axis orientation in polyethylene is usually attributed could take place. The easiest explanation for the observed phenomena would be a separation between PEHD and iPP on the length scale of a spherulite.

SAXS curves taken with a Paar Kratky compact camera and a Braun linear position-sensitive detector only show a broad shoulder from which the period of the apparently distorted lamellar stacking of crystalline and amorphous lamellae can be estimated to about 17 nm in the case of PEHD and 12 nm in the case of iPP. The SAXS curve of the blend closely resembles the measurement for PEHD.

Molecular modelling

Since it is known from experimental results that at temperatures below crystallization temperatures of iPP and PEHD their blends are semicrystalline materials, we assume the existence of all three types of interfaces: amorphous/amorphous, crystalline/crystalline and amorphous/crystalline. These three types of interfaces were created on the molecular level.

Concerning the crystalline/crystalline interfaces we refer to the configuration established in the literature: epitaxially crystallized high density PE on iPP or iPP on PE show the well defined 'cross-hatched' morphology[12–15]. Epitaxial growth has been carried out by two methods: (a) annealing of drawn blends of PE/iPP or sandwiched films of PE/iPP; and (b) vacuum deposition or cast film crystallization of PE or iPP onto single crystals or oriented film of iPP or PE, respectively. PE or iPP chains were inclined at a specific angle of about 50° to the substrate chain axes. The contacting planes were established to be (100)PE and (010)iPP, respectively. It is a straightforward interpretation that epitaxially grown PE chains interact with rows of methyl groups that populate the (010) plane of the iPP α-crystal, since PE chains fit exactly into the valleys formed by the methyl groups. However, it was not possible to determine experimentally which (010)PP plane, the one with higher or lower density of methyl groups[12], interacts with the (100)PE plane. While the structure of the PE/iPP interface was established in the case of epitaxial crystallization, experimental investigation of interfaces in the material made by technical blending meets problems in finding PE/iPP relationships. Since epitaxy is also very likely in the technical material we have investigated crystalline/crystaline interfaces of the (100)PE/(010)iPP–low density of methyl groups and (100)PE/(010)iPP–high density of methyl groups with four different orientations of the PE chains: at 0°, 90°, 46.8°, −46.8° with respect to the iPP chain axis. The 46.8° angle corresponds to the case of lattice matching of PE chains into the valleys formed by the methyl groups of iPP.

From the trajectories generated, we computed energies of adhesion. Computation of the crystalline PE and PP surface energies were carried out for the (100) and (010) crystallographic planes respectively: 2.97×10^{-1} J/m^2 for PE and

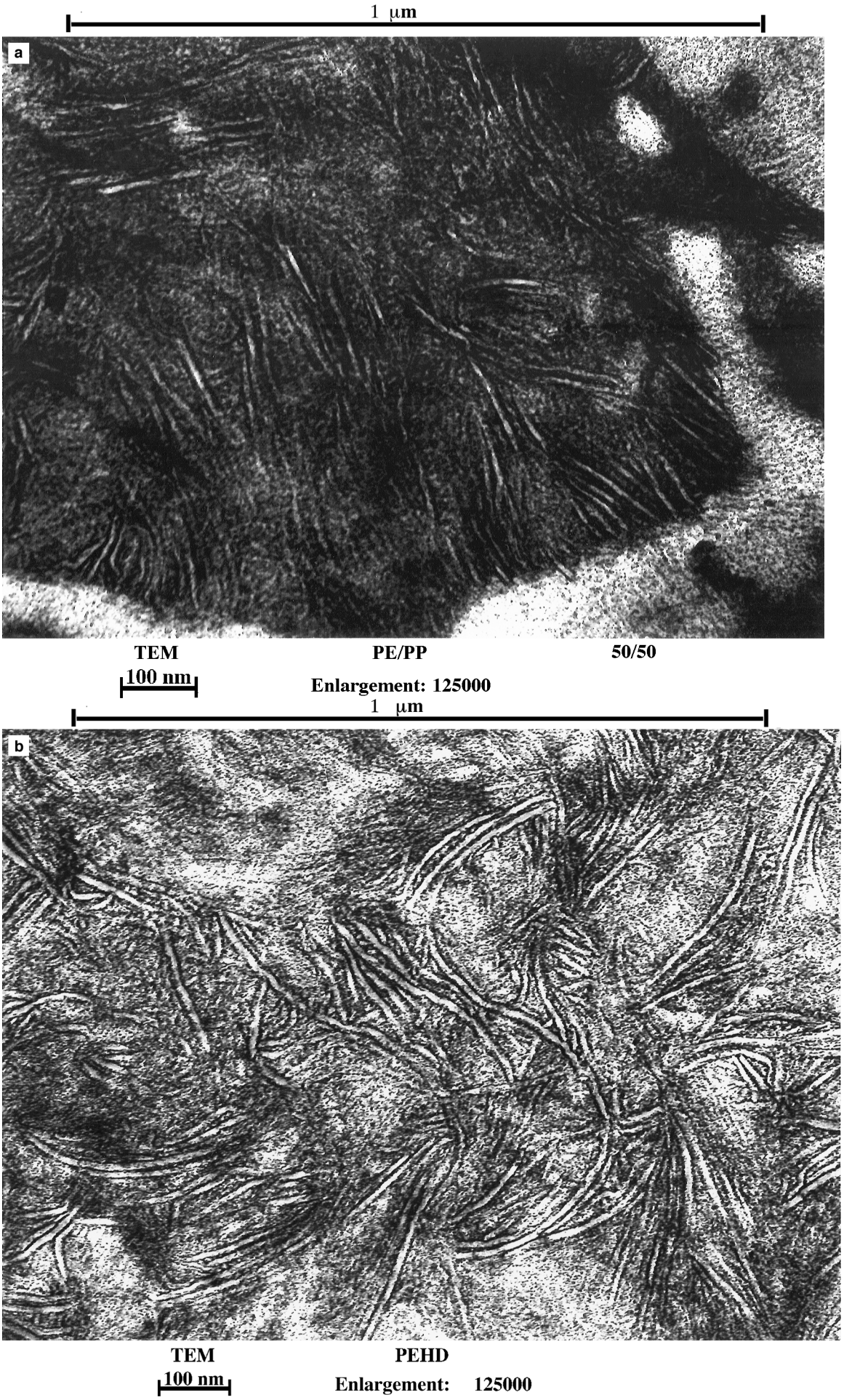

Figure 6 Transmission electron micrographs of (a) the 50/50 iPP/PEHD blend sample and (b) the pure PEHD sample

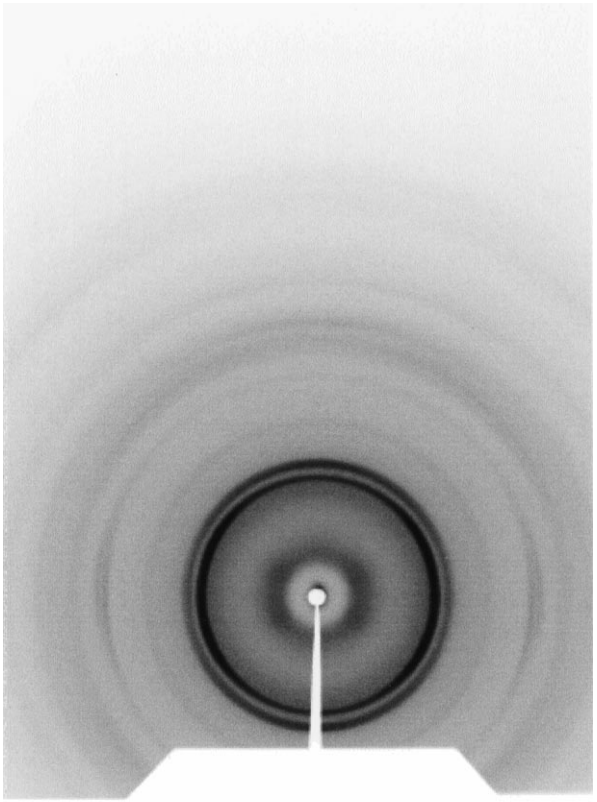

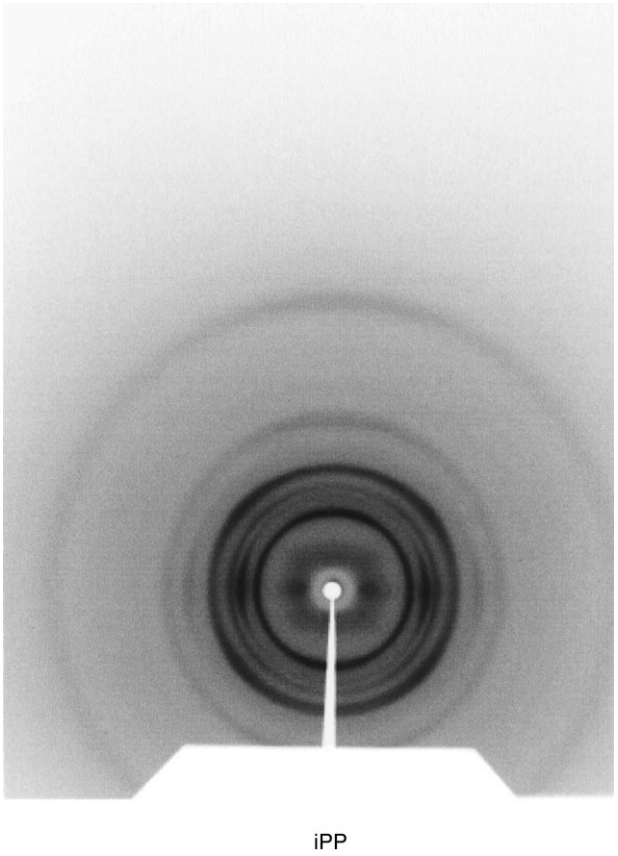

Figure 7 X-ray scattering pattern of the pure PEHD sample: (a) the crystallographic *b*-axis of the unit cell is oriented in the plane normal to the injection direction, the *a*- and *c*-axes are uniformally distributed about it; (b) X-ray scattering pattern of the iPP sample shows *c*-axis orientation; (c) the scattering diagram of the PEHD/iPP blend sample presents a superposition of the scattering patterns shown in (a) and (b)

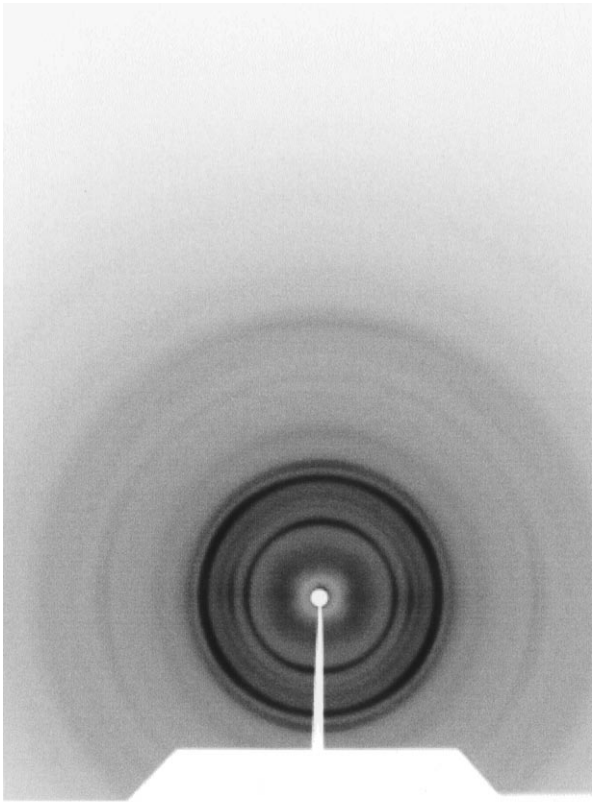

Figure 7 Continued.

1.4×10^{-1} J/m^2 for PP. Adhesion energies are summarized in *Table 1*.

Calculated surface energies for amorphous PE and PP are 2.65×10^{-1} J/m^2 and 1.3×10^{-1} J/m^2. Adhesion energy for the crystalline PP and amorphous PE is -1.8×10^{-1} J/m^2 for the interface of the crystalline PE and amorphous PP is 1.7×10^{-1} J/m^2.

Experimentally measured energies for the polypropylene/polyamide-6 interface rupture[16], containing diblock copolymer of PP/PA6 were reported in the range 1–100 J/m^2. In the case of the real macroscopic interface, macromolecules of one component interpenetrate into the second phase, and the strength of the interface depends strongly on the depth of this penetration. When a copolymer is added to the mixture of immiscible components, the strength of the interface is influenced by the length of the copolymer. In the case of computer simulation, interpenetration of one phase into another is not taken into account, reducing the calculated adhesion energy drastically. But in the case of epitaxial crystallization of the PE on the crystalline base of iPP, interpenetration of PE into iPP should not be expected and computer simulation should give true adhesion energies for this case.

The Gibbs energy of mixing ΔG_m could be estimated from $A(E_c - E_1 - E_2)/S$, where A is the total area of all interfaces in the blend, E_c is the energy of the combined system and E_1 and E_2 are the energies of each component building the interface. As long as we do not know A, which depends strongly on the preparation conditions, we can just consider the sign of ΔG_m: in all cases it is definitely positive, which means that PE and iPP are immiscible polymers even in the case of epitaxial crystallization.

Table 1 Summary of adhesion energies in J/m^2

Angle (°)	$E_1 + E_2 - E_c$ HD	$E_1 + E_2 - E_c$ LD	E_{adh} HD	E_{adh} LD
90	0.43	0.39	−0.01	−0.05
0	0.55		0.11	—
46.8	0.36	0.27	−0.08	−0.17
−46.8	0.55	0.49	0.11	0.5

LD means that (100)PE plane interacts with (010)iPP plane with low density of methyl groups, HD means that (100)PE plane interacts with (010)iPP plane with high density of methyl groups

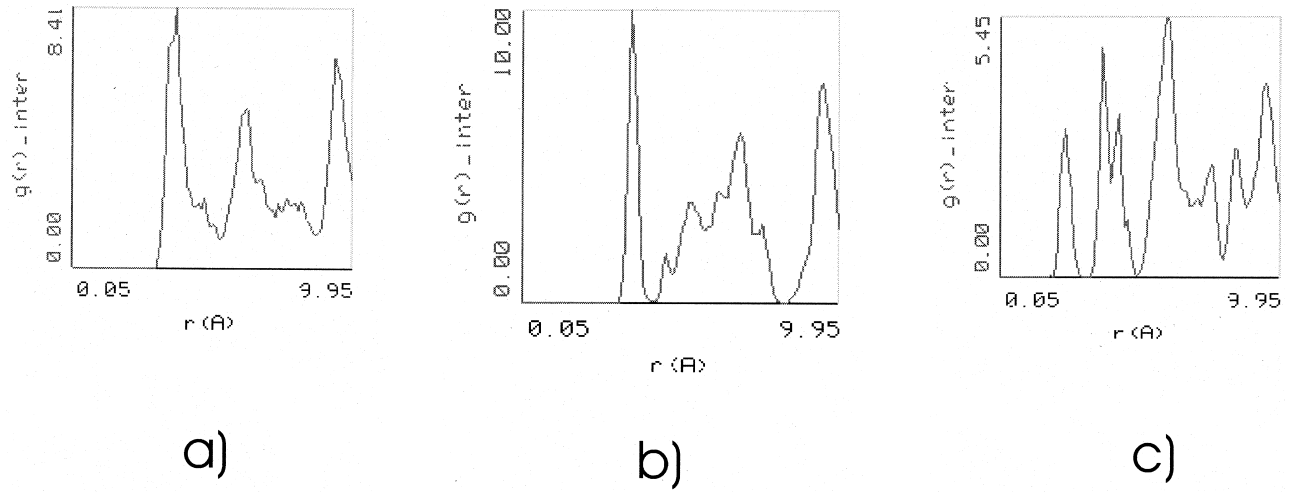

Figure 8 Pair distribution functions of the carbon atoms of the methyl groups calculated (a) within the first layer of iPP at the interface, (b) within the third layer and (c) within the a layer of the pure crystalline iPP

PE and iPP will tend to form the blend with the lowest free energy or lowest Gibbs energy. The choice between free energy or Gibbs energy depends on whether we run MD under the constant volume, temperature or constant pressure, temperature conditions. That means that PE and iPP should tend to form an interface with lowest interfacial energy. As can be derived from the MD calculation the system of PE chains rotated by 46.8° with respect to the iPP chain axes within the (010) plane with low density of methyl groups has the lowest adhesion energy. Of course we cannot insist on this because we could not investigate all possible angles of the rotation of the PE chains to the PP chains. But taking into account that experiments of the epitaxial crystallization of PE on iPP show that PE crystallizes at approximately 50° with respect to the PP chain axes, we will force our efforts on the investigation of the PE/iPP interphase with PE chains oriented at 46.8° to the direction of the iPP chain axes which corresponds to the model of epitaxial crystallization. Mismatching of angles could be explained by the difference in the experimental and calculated cell sizes of PE and iPP simple crystal cells.

In the following an interphase is defined by a volume consisting of two assembled molecular systems, where the structure of the molecules within a specific region is changed due to the interaction with the neighbourhood of different type. To visualise structural changes in the interphase pair distribution functions of carbon atoms in pure materials and in the interface region were computed. Comparing the pair distribution functions of the carbon atoms of the methyl groups within the crystalline iPP and at the interface (*Figure 8a–c*) of the combined system we find the structure altered within a layer of 3 nm thickness. This perturbation in the structure displayed in *Figures 9 and 10*

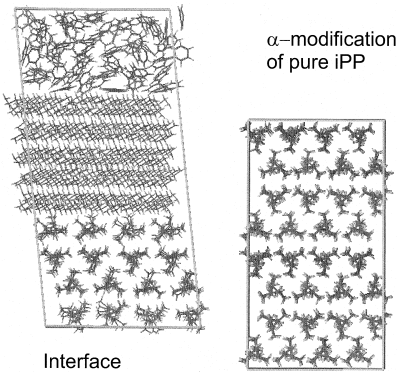

Figure 9 Interface of crystalline PE and crystalline iPP viewed along the molecular axis of the iPP molecules. The chain axes of the PE and iPP molecules are oriented by 46.8° with respect to each other

appears in both crystalline—PE and iPP—ensembles at the interface. However, the main effect in the PE/iPP interface is a structural change of the orthorombic PE crystal structure to monoclinic (*Figure 10*). This transformation already takes place during minimization and the monoclinic structure stays over the whole MD runtime of 500 ps. This monoclinic structure can be described in the following way. The PE molecules of the second layer (counted from the iPP(010) low density methyl face) performed a rotation about their molecular axes, ending up in the same orientation as the molecules of the first layer. The same process takes place in each even-numbered layer.

For the amorphous/amorphous interfaces a layer thickness of about 2 nm can be estimated.

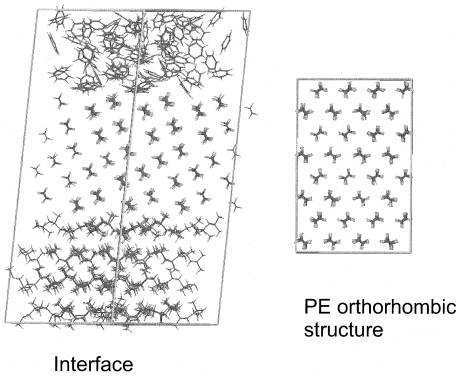

Figure 10 Interface of crystalline PE and crystalline iPP viewed along the molecular axes of PE. The PE molecules are oriented at 46.8° with respect to the molecular axes of the iPP molecules. Compared to the orthorhombic structure of the pure PE crystal the molecular chains in every other layer are rotated by about 90°, finally building a monoclinic structure

CONCLUSION

The impact strength of the investigated PEHD/iPP blend is correlated to the increased interphasial volume, caused by a specific processing which leads to an excellent distribution of nucleation centres. Contrary to the PEHD/iPP blend prepared by solution casting and imaged in a thin film by SFM, the PEHD/iPP injection moulded test piece does not contain the typical iPP spherulites, but is a bicontinuous network, as determined by TEM. Concerning the expitaxial crystalline/crystalline interphase of PEHD and iPP, MD calculations predict the energetically most favourable ensemble: a monoclinic structure of PEHD in contact with iPP. Furthermore, the (010)iPP contact plane, containing the low density of methyl groups, turns out to be more stable than the one with the high density of methyl groups.

ACKNOWLEDGEMENTS

U.N. is grateful to Dr W. Heckmann and Dr Frechen of BASF AG, Ludwigshafen, Germany, for providing the TEM images.

REFERENCES

1. Teh, J. W., *J. Appl. Polym. Sci.*, 1983, **28**, 605.
2. Teh, J. W., Noordin, R. and Low, A. K. Y., *Proc. Inst. Plast. Conf.*, Kuala Lumpur, Malaysia, 1985.
3. Krause, S., *Polymer Blends*, Vol. 1. Academic Press, New York, 1978, p. 15.
4. Solc, K., *Polymer Compatibility and Incompatibility Principles and Practices*. Harwood, New York, 1982.
5. The, J. W., *Proc. Int. Plast. Conf.*, Kuala Lumpur, Malaysia, 22 October 1985.
6. Plochocki, A. P., *Polymer Blends*, Vol. 2, ed. D. R. Paul and S. Newman. Academic Press, New York, 1978, pp. 319–368.
7. Last, A. G. M., *J. Polym. Sci.*, 1959, **39**, 543.
8. DISCOVER Version 3.2, Biosym Technologies Inc., San Diego, CA.
9. Berendsen, H. J.C., Postma, J. P. M., van Gunsteren, W. F., Dinola, A. and Haak, J. R., *J. Chem. Phys.*, 1984, **81**, 3684.
10. Tadokoro, H., *Structure of Crystalline Polymers*. Wiley-Interscience, New York, 1979.
11. Parrinello, M., *J. Appl. Phys.*, 1981, **52**, 7182.
12. Lotz, B. and Wittmann, J. C., *J. Polym. Sci., Part B*, 1986, **24**, 1559–1575.
13. Lotz, B. and Wittmann, J. C., *J. Polym. Sci., Part B*, 1987, **25**, 1079–1087.
14. Lee, I.-H. and Schultz, J. M., *J. Mater. Sci.*, 1988, **23**, 4237–4243.
15. Kawaguchi, A., Okihara, T., Murakami, S., Ohara, M., Katayama, K.-I. and Petermann, J., *J. Polym. Sci., Part B*, 1991, **29**, 683–690.
16. Boucher, E., Folkers, J. P., Hervet, H., Leger, L. and Creton, C., *Macromolecules*, 1996, **29**, 774.